Analytica Chimica Acta 1142 (2021) 127–134

Contents lists available at ScienceDirect

Analytica Chimica Acta

journal homepage: www.elsevier.com/locate/aca

3D matrixed DNA self-nanocatalyzer as electrochemical sensitizers for ultrasensitive investigation of DNA 5-methylcytosine

Quanjing Zhu [a, 1], Haoyang Yang [a, 1], Jing Luo [a], Hui Huang [a], Lichao Fang [a], Jun Deng [a], Chenghong Li [a], Yan Li [a, **], Tao Zeng [b, c, ***], Junsong Zheng [a, *]

[a] Department of Clinical and Military Laboratory Medicine, College of Medical Laboratory Science, Army Medical University, 30 Gaotanyan Street, Shapingba District, Chongqing, 400038, PR China
[b] Department of Medical Laboratory, Affiliated Hospital of Guangdong Medical University, Zhanjiang, Guangdong, 524000, PR China
[c] Department of Medical Laboratory, School of Laboratory Medicine and Biotechnology, Southern Medical University, Guangzhou, Guangdong, 510515, PR China

HIGHLIGHTS

- A novel ultrasensitive electrochemical strategy was developed for DNA 5-methylcytosine detection.
- The proposed novel electrochemical sensitizers to achieve signal amplification, which was superior to most current methods.
- The new AuNPs/g-C_3N_4@rGO nanocomposites can further improve the electrochemical performances of the bioassay.
- The proposed strategy provides a new avenue for early diagnosis of methylation-related diseases.

GRAPHICAL ABSTRACT

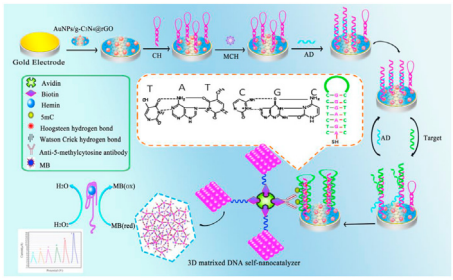

ARTICLE INFO

Article history:
Received 3 June 2020
Received in revised form
27 September 2020
Accepted 31 October 2020
Available online 5 November 2020

Keywords:
DNA 5-Methylcytosine
Self-nanocatalyzer
Electrochemical biosensor
3D matrix
Triple-helix
AuNPs/g-C_3N_4@rGO nanocomposites

ABSTRACT

DNA methylation plays an important role in a variety of human diseases. Thus, accurately analyze 5-methylcytosine in different DNA segments is of great significance. Herein, we proposed a novel 3D matrixed DNA self-nanocatalyzer *via* gold nanoparticles (AuNPs) supporting DNA self-hybridization with hemin as biomimetic enzyme and methylene blue (MB) as electrochemical mediator, which was employed as an efficient electrochemical sensitizer for the ultrasensitive bioassay of DNA 5-methylcytosine. Meanwhile, the AuNPs, graphitic carbon nitride (g-C_3N_4) and reduced graphene oxide (rGO) was prepared as AuNPs/g-C_3N_4@rGO nanocomposites to coat on the electrode surface to immobilize the capture hairpin DNA (CH). In the presence of target DNA with 5-methylcytosine, the target DNA could hybridize with CH *via* the hyperstable triple-helix formation. Based on the specific biorecognition between biotin and streptavidin and immune recognition between anti-5-methylcytosine antibodies and 5-methylcytosine sites on the target DNA, the 3D matrixed DNA self-nanocatalyzer could be captured onto the electrode surface to generate an amplified electrochemical signal related to the concentration of 5-methylcytosine. Under the optimal conditions, the proposed strategy performed a linear range from 10^{-17} M to 10^{-8} M with a detection limit of 8.6 aM. Remarkably, this strategy could be expanded easily to

* Corresponding author. Department of Clinical and Military Laboratory Medicine, College of Medical Laboratory Science, Army Medical University, 30 Gaotanyan Street, Shapingba District, Chongqing, 400038, PR China.
** Corresponding author.
*** Corresponding author. Department of Medical Laboratory, Affiliated Hospital of Guangdong Medical University, Zhanjiang, Guangdong, 524000, PR China.
E-mail addresses: liyanlwb1003@126.com (Y. Li), zengt@smu.edu.cn (T. Zeng), zhengalpha@sina.com (J. Zheng).
[1] Equal contribution by the first two authors.

https://doi.org/10.1016/j.aca.2020.10.064

various biomarkers, including protein, DNA, phosphorylation and glycosylation, providing a promising strategy for clinical diagnosis and mechanism investigation of various diseases.

1. Introduction

DNA methylation as one of the major epigenetic modification catalyzed by methyltransferase involving the addition of a methyl group (-CH_3) to the C-5 position of the cytosine nucleotide named as 5-methylcytosine [1,2]. Many researchers are continuously uncovering the important role of DNA methylation in a variety of human aging, tumorigenesis, and other genetic and epigenetic diseases [3,4], such as auto-immune diseases, metabolic disorders, leukemia, lung cancer, and colon cancer. It is of great significance to the early diagnosis and treatment that accurately analyze methylation in different DNA segments [5]. Recently, many techniques have been developed to measure 5-methylcytosine including bisulfite conversion-based or methylated DNA immunoprecipitation (MeDIP)-based PCR or sequencing [6,7]. Bisulfite conversion is a popular technique to prepare DNA for methylation analysis, in which cytosine is converted to uracil *via* sodium bisulfite, while 5-methylcytosine remains unaffected. Followed by the conversion, the prepared samples were detected on a gene-specific level based on PCR or sequencing to calculate the DNA methylation of the target gene. Whereas the chemical reaction conditions should be optimized carefully because the harsh chemical reaction often degrades the DNA. MeDIP is a non-invasive detection technique *via* immune recognition between anti-5-methylcytosine antibodies and 5-methylcytosine sites on the target DNA fragments, which normally process with an amplification technique to detect the sequence-specific DNA methylation, including PCR and sequencing. However, these traditional methods generally limited with the complicated analysis procedures, costly instruments and low sensitivity for the widely applied to clinical diagnosis. It is extremely important and urgent to establish a simple, stable, convenient way to analyze the DNA 5-methylcytosine for clinical diagnosis and mechanism investigation of various diseases.

Currently, electrochemical biosensors have attracted considerable attention due to their significant advantages, such as quick response, low cost, and convenient operation, which have been successfully employed in some clinical applications [8,9]. In the electrochemical systems, the electrochemical mediators were normally labeled onto the proteins or nucleotides as signal probes, in which the electrochemical responses could be improved easily by increasing the electrochemical mediators with the help of nanomaterials, e.g. doping in the nanoparticles, coating on the surface of the nanoparticles [10,11]. It's efficient and convenient. Recently, Hua and coworkers reported a simple approach with DNA-based nanostructure to loading amounts of methylene blue (MB) as electrochemical mediators *via* the stable conjugation between double-stranded DNA and MB for the sensitive detection of DNA inside living cells [12]. Very recently, we proposed a sensitive electrochemical strategy by the target-induced hybridization chain reaction (HCR) and rolling circle amplification (RCA) to produce massive double stranded DNA to immobilize doxorubicin-dicarboxyferrocene as electrochemical mediators, in which the large interspace among DNA chains were useful for the electron transfer to generate higher electrochemical responses [13]. On the other hand, the enzyme-substrate system was employed in the electrochemical assay to increase the reaction efficiency of electrochemical mediator significantly, in which the horseradish peroxidase (HRP)/H_2O_2 as the common system was widely employed in the clinical diagnosis [14]. With the rapid development of the enzyme, various new enzymes were proposed to improve their efficiency and application, especially the DNA-based biomimetic enzyme with higher stability and efficiency [15]. G-quadruplex (G4) DNAzymes with the cofactor hemin has attached much attention as one of the efficient peroxidase-mimicking biomimetic enzymes, which has been widely employed in various clinical diagnostic platforms [16,17]. In order to improve the loading amounts of G4 DNAzymes, they were usually loaded onto nanomaterials (NMs) to fabricate DNA-NMs constructs acting as catalytic labels. Thus, taking the advantages and challenges of electrochemical biosensor into consideration, it could be expected that a highly improved amplification efficiency by combining the high efficient loading techniques and catalytic approaches [18,19].

In this study, we proposed a novel 3D matrixed DNA self-nanocatalyzer *via* AuNPs supporting DNA self-hybridization with hemin in the G4 structure as biomimetic enzyme and methylene blue (MB) inset in the double-stranded structure as electrochemical mediator, which was employed as an efficient electrochemical sensitizer for the ultrasensitive bioassay of DNA 5-methylcytosine (see Scheme. 1). Typically, DNA linker A, DNA linker B, G4 DNA and biotin labeled linker C were immobilized onto the two AuNPs, and the 3D matrixed DNA self-nanocatalyzer was constructed by the hybridization between DNA linker A and DNA linker B, and immobilization a great deal of hemin to form biomimetic enzyme and MB as electrochemical mediator in the 3D DNA matrix. Thus, the hemin could catalyze the reaction of MB with H_2O_2 and amplify the electrochemical response of MB for ultrasensitive electrochemical assay. In order to improve the electrochemical performances of the bioassay, the AuNPs, graphitic carbon nitride (g-C_3N_4) and reduced graphene oxide (rGO) was prepared as new AuNPs/g-C_3N_4@rGO nanocomposites with good electronic transmission performance and large surface area to coat on the electrode surface as support matrix to immobilize the capture hairpin DNA (CH) [20,21]. In the presence of target DNA with 5-methylcytosine, the target DNA could hybridize with CH with the help of assist DNA (AD) *via* the hyperstable triple-helix formation [22]. Based on the specific biorecognition between biotin and streptavidin, and immune recognition between anti-5-methylcytosine antibodies and 5-methylcytosine sites on the target DNA, the 3D matrixed DNA self-nanocatalyzer could be immobilized onto the electrode surface to generate an amplified electrochemical signal for quantitative detection of DNA 5-methylcytosine. Remarkably, this proposed strategy with 3D matrixed DNA self-nanocatalyzer could be easily expanded to various biomarkers, such as protein, DNA, phosphorylation and glycosylation, providing a new route for clinical diagnosis and mechanism investigation of various diseases.

2. Experimental

2.1. Reagents and materials

G-C_3N_4 was obtained from Macklin Biochemical technology (shanghai, China). Hydrazine, graphene oxide (GO), MB, ammonia (25%), dimethyl sulfoxide (DMSO), 6-mercaptoethanol (MCH) and hemin were purchased from Sigma Chemical Co., USA. The BBI Life

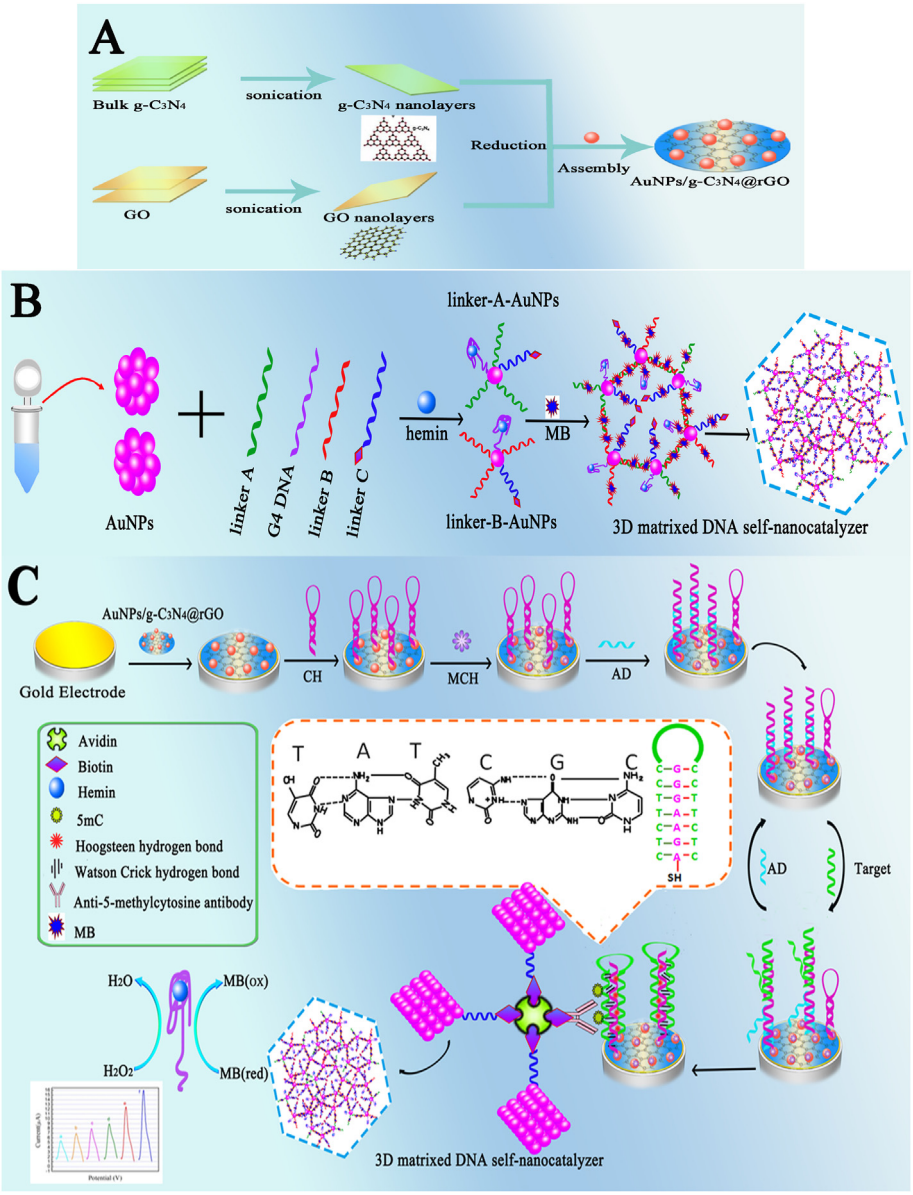

Scheme 1. Schematic illustration of the electrochemical assay for DNA 5-methylcytosine with 3D matrixed DNA self-nanocatalyzer as signal amplification strategy. (A) preparation process of AuNPs/g-C_3N_4@rGO nanocomposites; (B) preparation process of the 3D matrixed DNA self-nanocatalyzer; (C) fabrication process of the electrochemical biosensors.

Sciences Corporation supplied the tris (2-carboxyethyl) phosphine hydrochloride (TCEP, 98%). Chloroauric acid ($HAuCl_4$) was acquired from J&K Chemical (Beijing, China). The biotinylated anti-5-methylcytosine antibody was provided by Abcam (Cambridge, MA, USA). Phosphate-buffered saline (PBS), hydrogen peroxide (H_2O_2), Tris-ethylenediaminetetraacetic acid buffer (TE, pH 8.0), trisodium citrate, 4-(2-hydroxyethyl)-1-piperazineethanesulfonic acid (HEPES), streptavidin, sodium borohydride ($NaBH_4$), and all the oligonucleotides (Table S1) were obtained from Sangon Biotechnology Co., Ltd. (Shanghai, China). The gold electrodes ($\varphi = 3$ mm) were purchased from Aida Hengsheng Technology Co., Ltd. (Tianjin, China). All chemical reagents were analytical reagent. Ultrapure water (18.2 MΩ cm^{-1}) was used in all aqueous solutions.

2.2. Apparatus

Electrochemical impedance spectroscopy (EIS), differential pulse voltammetry (DPV) and cyclic voltammetry (CV) were measured on electrochemical workstation (CHI660E, Shanghai CH Instruments, China) based on a traditional three-electrode system with a saturated silver chloride electrode as the reference electrode, a gold electrode as the working electrode and a platinum wire as the auxiliary electrode. The morphology of the synthetic nanocomposites and 3D matrixed DNA network were characterized by the Fourier Transform Infrared (FT-IR) Spectrometer (Thermo Fisher, USA), X-ray photoelectron (XPS) spectroscopy (Thermo Fisher, USA), atomic force microscopy (AFM) (IPC–208B, Chongqing University), and field emission transmission electron microscope (TEM) (Thermo Fisher Scientific CD Ltd, Holland) operating at 200 kV accelerating voltage. Circular dichroism (CD) spectrograph (Chirascan, Applied Photophysics Ltd. England) was used to illustrate the conformations of the triple helix in a range of 200–320 nm at 18 °C with a response time of 5 s and the scanning speed of 120 nm/min. Multiskan Sky Microplate Spectrophotometer (Thermo Fisher Scientific, China) was

used to estimate the feature of AuNPs and 3D matrixed DNA networks.

2.3. Preparation of AuNPs/g-C_3N_4@rGO nanocomposite

AuNPs/g-C_3N_4@rGO nanocomposites were prepared according to the previous works with a slight modification [23,24]. Firstly, GO (50 mg) was diluted to 0.5 mg mL^{-1} suspension with ultrapure water and dispersed by ultrasonication for 1 h 1 mg g-C_3N_4 was dissolved into 1 mL ultrapure water and ultrasonicated for 4 h. Subsequently, the redundant g-C_3N_4 was abandoned by centrifugation at 2000 rpm for 30 min, and the top liquid, the g-C_3N_4 nanolayers aqueous suspension, was collected. Next, 18 mL GO solution and 1 mL g-C_3N_4 nanolayer suspension were mixed and diluted into 100 mL to form g-C_3N_4@GO suspension. And then, 350 μL of ammonia (25%) and 40 μL of hydrazine was added into the g-C_3N_4@GO suspension, and the mixture was sonicated for 1 h and magnetically stirred for 5 h at 100 °C, respectively, to reduce the g-C_3N_4@GO to g-C_3N_4@rGO suspension. Subsequently, 10 μL of 0.1 M $HAuCl_4$ solution was added to 4 mL g-C_3N_4@rGO suspension after sonicated 15 min, and the solution was continuously stirred at 85 °C. Next, 30 μL 0.08 M freshly made $NaBH_4$ solution and 10 μL of 0.01 M sodium citrate solution was quickly injected to reduce the $HAuCl_4$ with continuous stirring for 25 min. After centrifugation thrice to remove excess ingredients, the obtained AuNPs/g-C_3N_4@rGO nanocomposites were dispersed in ultrapure water.

2.4. Preparation of the 3D matrixed DNA self-nanocatalyzer

Gold nanoparticles (AuNPs) were prepared as a classic method described [25]. Firstly, 100 mL of 0.01% (w/v) $HAuCl_4$ solution was boiled with vigorous stirring, and then 4 mL of 1% (w/v) trisodium citrate solution was added quickly into the boiling solution with continuous stirring for 10 min. When the color of the solution changed to wine red, the AuNPs were obtained. After cooling to room temperature, store the solution in brown glass bottles at 4 °C for future use.

The 3D matrixed DNA self-nanocatalyzer was obtained based on the previous references with slight modification [26]. Firstly, TCEP was used to activate the thiolated DNA linker A, DNA linker B, G4 DNA and biotin labeled linker C, respectively. And then, 500 μL AuNPs solution was mixed with 15 μL 100 μM linker A, linker C and G4 DNA at 4 °C for 16 h to prepare DNA linker A-AuNPs, and 500 μL AuNPs solution was mixed with 15 μL 100 μM linker B, linker C, and G4 DNA at 4 °C for 16 h to prepare DNA linker B-AuNPs, respectively. And then, 10 μL of 1% SDS was injected into the mixture at room temperature with gentle shaking about 1 h, and 50 μL 0.5 M NaCl solution was slowly added into the mixture to age the DNA linker A-AuNPs and DNA linker B-AuNPs for 12 h. After washing centrifugation thrice with 0.01 M PBS (4 °C, 20 min, and 12,000 rpm), 500 μL 25 mM HEPES buffer solution containing 200 mM NaCl, 20 μM hemin, 20 mM KCl, 1% DMSO, and 0.1% Triton X-100 was mixed into the precipitant at 25 °C for 60 min to form the G-quadruplex with hemin as coreactor [27]. After washing, the mixture was redispersed in 500 μL 0.01 M PBS (20 μM MB, 20 mM KCl, pH 7.4) and stored at 4 °C. The construction of the 3D matrixed DNA self-nanocatalyzer was implemented by hybridization between DNA linker A-AuNPs and DNA linker B-AuNPs (37 °C, 2 h).

2.5. Fabrication of the electrochemical biosensors

The gold electrode was carefully burnished with 0.05 and 0.3 μm alumina powder and sonicated in ultrapure water, acetone and ultrapure water for 5 min, respectively. And then, the electrode was activated by freshly prepared piranha solution (30% H_2O_2: 98% H_2SO_4 = 1:3) for 15 min, cleaned with distilled water and dried with nitrogen thoroughly. Afterward, 10 μL AuNPs/g-C_3N_4@rGO solutions were dropped onto the electrode surface and dried in air at room temperature. Next, 10 μL of thiol-modified CH was assembled on the AuNPs/g-C_3N_4@rGO nanosheet surface at 4 °C for overnight to immobilize CH on AuNPs *via* Au–S affinity. After washing with ultrapure water to remove the free probe, the electrode was soaked in 15 mL 2 mM MCH solution at room temperature for 1 h to block nonspecific binding sites. Additionally, the fabrication of the electrochemical biosensor was characterized by EIS and CV in 15 mL 2 mM and 5 mM $[Fe(CN)_6]^{3-/4-}$ solution with 0.1 M KCl, respectively.

For the detection of target DNA 5-methylcytosine, 10 μL of the mixture with target DNA and AD was dripped onto the prepared biosensor for 150 min at 37 °C to form the target DNA-based triple-helix DNA structure. Then, 10 μL of biotinylated anti-5-methylcytosine antibodies (10 μg mL^{-1}) were dropped on the electrode surface for 1 h at 37 °C. Subsequently, the biosensor was submerged in 10 μg mL^{-1} streptavidin solution at 37 °C for 40 min. Finally, the biosensor was immersed in the solution with 3D matrixed DNA self-nanocatalyzer for 40 min at 37 °C. After washing with PBS, the biosensor was characterized based on the DPV technique with a potential range from −0.6 V to 0.1 V and pulse amplitude of 50 mV in 15 mL of 0.1 M PBS (2.5 mM H_2O_2, 0.1 M KCl).

3. Results and discussion

3.1. Characterizations of AuNPs/g-C_3N_4@rGO nanocomposites

The morphology of AuNPs/g-C_3N_4@rGO was characterized by TEM. As shown in Fig. 1, the GO (Fig. 1A) and g-C_3N_4 (Fig. 1B) were planar sheet-like, illustrating that the nanosheets were successfully dispersed. Under the interplay of the π-π stacking and electrostatic attraction, the rGO and g-C_3N_4 formed the g-C_3N_4@rGO film (Fig. 1C). Meanwhile, the AuNPs were modified on the g-C_3N_4@rGO film tightly and uniformly, which constituted the AuNPs/g-C_3N_4@rGO (Fig. 1D) nanocomposites. Besides, the FT-IR spectra and XPS were also used to characterize the composite materials (Figs. S2–S3).

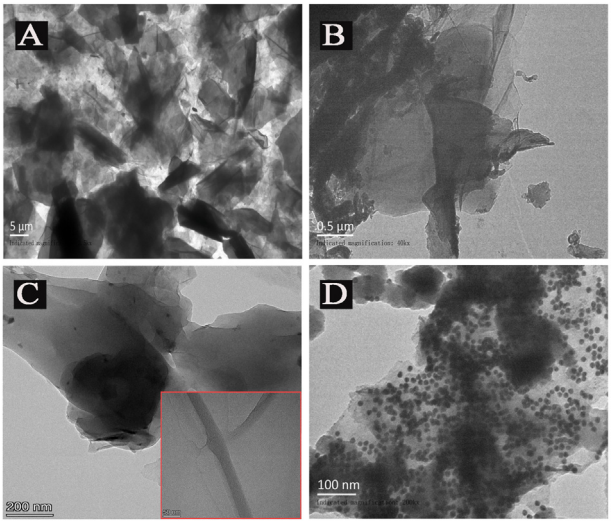

Fig. 1. TEM images of (A) GO, (B) g-C_3N_4, (C) g-C_3N_4@rGO (inset shows the HRTEM image), (D) AuNPs/g-C_3N_4@rGO.

3.2. Characterizations of 3D matrixed DNA self-nanocatalyzer

The morphology of 3D matrixed DNA network was characterized by AFM and TEM. The AFM image of pure AuNPs is exhibited in Fig. 2A, in which white dots were the AuNPs. Fig. 2B clearly shows that the morphology of DNA linkers-AuNPs, when the 3D matrixed DNA network was formed, the AFM image shows that the spherical spatial structure (Fig. 2C). Similarly, it can be seen that the AuNPs were uniformly distributed with a diameter of about 16 nm under the TEM (Fig. 2D). In Fig. 2E, many nanoparticles are linked by DNA to form a network structure. In addition, the Uv–vis absorption spectrum also used to characterize the structure (Fig. 2F). DNA linker has presented a characteristic absorption peak at 260 nm (curve a), the bare AuNPs presented a characteristic absorption peak at 520 nm (curve b). After the decoration of DNA linkers on AuNPs, the AuNPs' absorption peak was shifted to 524 nm, the DNA linkers' absorption peak was shifted to 270 nm and the absorption intensity was decreased (curve c). When the DNA linker A-AuNPs was hybridized with DNA linker B-AuNPs, the absorption peak was a further red shift and absorption intensity decreased again (curve d). The results demonstrated that the 3D matrixed DNA self-nanocatalyzer was carried out successfully.

3.3. Electrochemical characterization of the biosensor

In this work, the fabrication process of the electrochemical biosensor was investigated based on CV and EIS measurements. CV measurements were performed in a 2 mM $[Fe(CN)_6]^{3-/4-}$ solution containing 0.1 M KCl. As Fig. 3A shows, the bare gold electrode performed a well-defined redox peak of $[Fe(CN)_6]^{3-/4-}$ (curve a). When the AuNPs/g-C_3N_4@rGO nanocomposites were modified on the gold electrode surface, leading to apparently increased of the peak current with a decreased oxidation-reduction potential (curve b), which could be mainly attributed to the good conductivity of AuNPs/g-C_3N_4@rGO and the effectively increased surface area to accelerate the electron transfer between the layers and gold electrode substrate. On the other hand, the nanocomposites changed the activation energy of the reactions on the electrode surface, resulting in a shift of peak potential. After the CH immobilized onto the surface of the electrode, the peak current was reduced obviously and the oxidation-reduction potential was increased obviously (curve c), which accounted for the electrostatic repulsion between the negatively charged CH strands and $[Fe(CN)_6]^{3-/4-}$ inhibited the diffusion of redox medium, indicating the successful immobilization of CH onto the gold electrode surface. When the

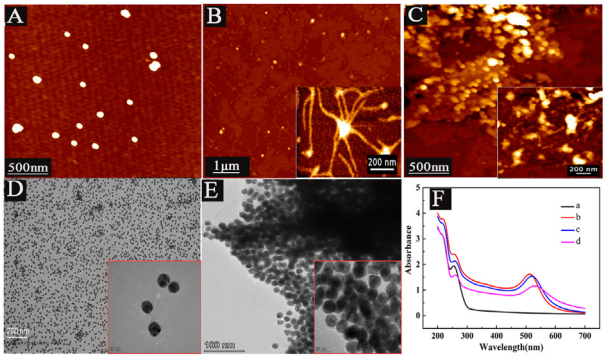

Fig. 2. AFM images of (A) AuNPs, (B) decoration of DNA linkers on AuNPs, (C) 3D matrixed DNA network. (D) TEM images of AuNPs (inset shows the HRTEM image), (E) 3D matrixed DNA self-nanocatalyzer (inset shows the HRTEM image). (F) UV–Vis absorption spectra of DNA linker (curve a), AuNPs (curve b), decoration of DNA linkers on AuNPs (curve c), 3D matrixed DNA network (curve d).

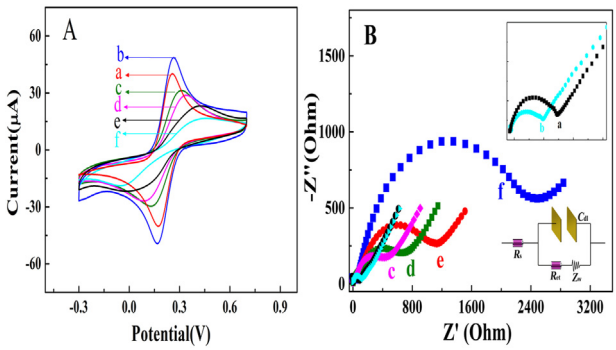

Fig. 3. (A) CV characterizations and (B) EIS characterizations for the fabrication of the biosensor. CV (−0.3 to 0.7 V and scan rate of 50 mV/s). EIS (5×10^{-2} to 1×10^{6} Hz). (a) Bare GE, (b) AuNPs/g-C_3N_4@rGO modified GE, (c) assembled CH on GE, (d) MCH/CH/AuNPs/g-C_3N_4@rGO/GE, (e) fabricated with AD and target DNA, (f) incubated with the 3D matrixed DNA network. (Inset shows the equivalent circuit diagram, in which Rs was the electrolyte resistance, C_{dl} was the double-layer capacitance, Ret was the electron transfer resistance and Zw was the Warburg impedance, respectively.).

nonconductive MCH employed to block non-adsorbed sites, the peak current was decreased obviously with a significantly increased oxidation-reduction potential (curve d) due to the inhibition of MCH for electron transfer. Then, the reaction with AD and target DNA, a further decreased of peak current, and an increased oxidation-reduction potential was observed (curve e). This could be mainly owing to the insulating behavior of the large sized of the immobilized DNA strands. When the biosensor reacted with the biotinylated anti-5-methylcytosine antibody and the 3D matrixed DNA network, the peak current dramatically decreased and oxidation-reduction potential increased again due to the increase of space steric hindrance blocking the charge transfer and diffusion between the solution and the electrode surface (curve f).

Additionally, the assembly processes of the electrode were characterized by EIS in 5 mM $[Fe(CN)_6]^{3-/4-}$ in a frequency range from 5×10^{-2} to 1×10^{6} Hz (Fig. 3B), in which the electron transfer resistance (R_{et}) was employed to demonstrate the electron transfer kinetics quantitatively. The R_{et} was accurately computed based on the model impedance data *via* the equivalent circuit (insert figure of Fig. 3B). The bare gold electrode showed excellent conductivity with the R_{et} value of 91.5 Ω (curve a). When the AuNPs/g-C_3N_4@rGO nanocomposites were deposited onto the electrode surface, the R_{et} was decreased to 55.3 Ω (curve b), which attributed to the conductive AuNPs/g-C_3N_4@rGO sheets increasing the surface area and accelerating the electron transfer. After the modification of CH, the R_{et} increased to 332 Ω (curve c). After blocking with MCH (curve d), the value increased again (R_{et} = 449 Ω). When the target DNA and AD were reacted with the biosensor, the R_{et} increased to 569 Ω (curve e) because of the hindrance of oligonucleotide on the electron transfer. After the anti-5-methylcytosine antibody and the 3D matrixed DNA network was modified on the electrode, the R_{et} value dramatically grew to about 2123 Ω (curve f). All of the CV and EIS measurements demonstrated the successful fabrication of the biosensor.

3.4. Comparison of different amplification strategies

In order to validate the signal amplification strategies of the proposed biosensor, the various strategies were utilized on a similar electrode with the same target DNA concentrations (Fig. 4). When the DNA linker A-AuNPs loaded with MB was incubated on the biosensors, the MB could selectively bind to G base on the ssDNA linkers as an electrochemical mediator, the DPV response was only about 2.75 μA (Fig. 4A). When the hemin was added to the

DNA linker A-AuNPs to formed G4 DNAzymes, which could catalyze the reaction of MB with H_2O_2 and amplify the electrochemical response, the current increased to 2.9 μA (Fig. 4B). After the 3D matrixed DNA network formed, the dsDNA linkers could load more MB as electrochemical mediators *via* the stable conjugation between double-stranded DNA and MB, so the electrochemical signal responses reached 4.2 μA (Fig. 4C). As Fig. 4D exhibited that DPV value was significantly enhanced to 5.3 μA with the hemin and MB coexists in the 3D matrixed DNA network. This could be mainly owing to the 3D matrixed DNA self-nanocatalyzer with amounts of the electronic mediator on the electrochemical biosensor surface and the efficient catalytic effect of hemin on the reaction of MB with H_2O_2 to amplify the electrochemical response of MB.

3.5. Optimization of experimental conditions

In the experiment, the important conditions for the electrochemical assay were optimized based on their electrochemical responses, including the pH of the solution, incubation temperature, incubation time, antibody concentration, hemin concentration, and H_2O_2 concentration, respectively. Firstly, in the triplex DNA system, the T-A•T and C-G•C^+ triplex were formed *via* the Hoogsteen hydrogen bonds, which was mainly related to the pH of the solution [28]. Herein, the effect of pH for the DPV responses was studied firstly. As shown in Fig. 5A, the DPV response initially increased and then decreased in pH range from 4 to 7, and the highest response was obtained at pH 5.5. Therefore, a pH of 5.5 was selected as the optimal solution pH in this study. Meanwhile, the temperature and reaction time is also important in the construct of triple-helix. As shown in Fig. 5B, in the temperature from 25 °C to 45 °C, a maximum DPV response was observed at 37 °C, illustrating that 37 °C is the optimal temperature. For the different reaction time for the triple-helix formation, the DPV response increased rapidly with the rise of the reaction time and reached a peak value when the reaction time was longer than 150 min (Fig. 5C). Thus, 150 min was selected as the optimal reaction time in this work. Additionally, the concentration of antibody as one of the critical factors in the immunoassay was optimized in this work with different concentrations of antibodies ranged from 0 μg mL^{-1} to 30 μg mL^{-1}. Seen Fig. 5D, the electrochemical responses increased with the concentration of antibody, and then reached a platform when the antibody concentration was higher 10 μg mL^{-1}. Therefore, 10 μg mL^{-1} was

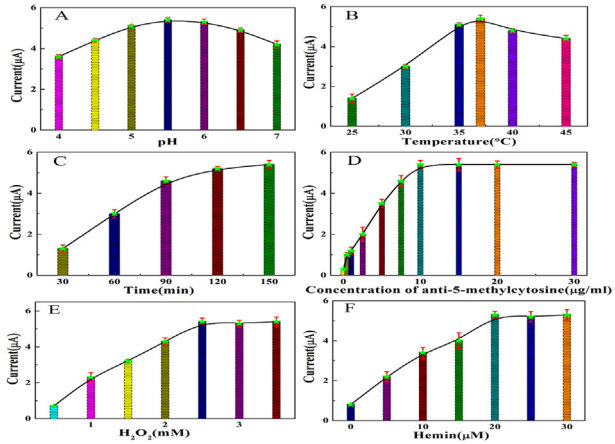

Fig. 5. Optimization for the electrochemical assay conditions. (A) The pH of the solution; (B) the reaction temperature for the triple-helix formation; (C) the reaction time for the triple-helix formation; (D) the concentration of the anti-5-methylcytosine antibody; (E) the concentration of H_2O_2; (F) the concentration of hemin.

selected as the optimized concentration of antibody in the experiment. Furthermore, the concentration of hemin and H_2O_2 was optimized based on the electrochemical responses with different concentrations of hemin and H_2O_2. As shown in Fig. 5E and F. The optimal concentration of H_2O_2 and hemin was 2.5 mM and 20 μM, respectively.

3.6. Application of the electrochemical biosensor in the assay of DNA 5-methylcytosine

In order to validate the feasibility of the proposed biosensor, the UT (unmethylated target DNA) detected firstly. As shown in Fig. 6, the DPV response was weak without 5-methylcytosine site (curve a). In contrast, an obvious oxidation peak could be obtained in presence of 5-methylcytosine site (Fig. 6 curve b), because the triple-helix structure contained a methyl group to recognize anti-5-methylcytosine antibody and binding 3D matrixed DNA self-nanocatalyzer to generate a significant electrochemical response, indicating the potential feasibility of the biosensor for the detection of DNA 5-methylcytosine.

In order to evaluate the application performances of the

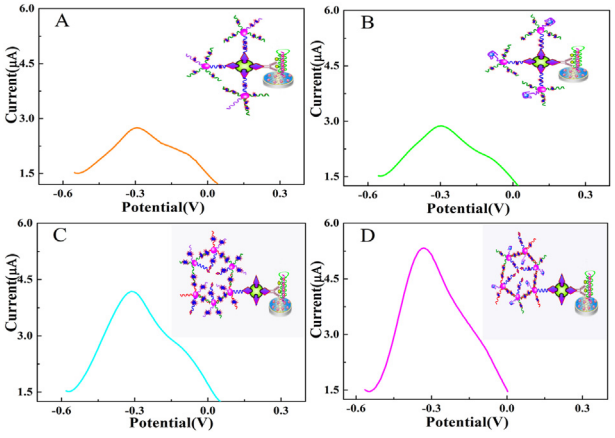

Fig. 4. Comparative study of different signal amplification methods based on DPV detection: (A) only incubated with the DNA linker A-AuNPs loaded with MB; (B) incubated with hemin and MB on the DNA linker A-AuNPs; (C) MB intercalated into the 3D matrixed DNA self-nanocatalyzer; (D) cooperative action of hemin and MB on the 3D matrixed DNA self-nanocatalyzer.

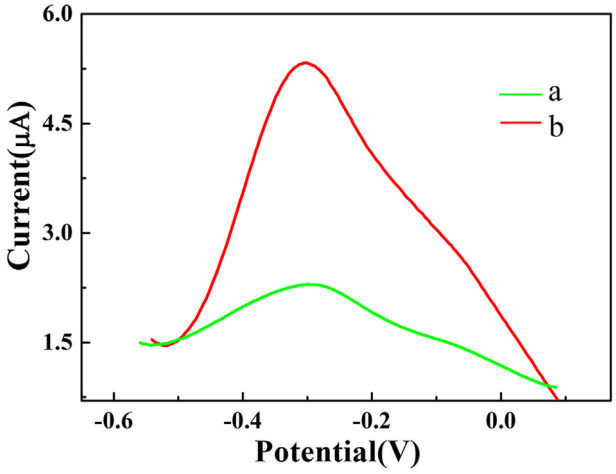

Fig. 6. DPV response to UT (curve a), and target DNA with 5-methylcytosine site (curve b).

proposed electrochemical bioassay, the electrochemical responses of target DNA were studied with various concentrations in the range from 10^{-17} M to 10^{-7} M. As Fig. 7A shows, the electrochemical response increased with the concentration of target DNA, which could be attributed more target DNA causing enhanced immobilization of anti-5-methylcytosine antibody and binding 3D matrixed DNA self-nanocatalyzer to generate an enzyme-based electrochemical reaction with the amount of electrochemical mediator, performing increased electrochemical signals related with the concentration of target DNA. As shown in Fig. 7B was the relationship between the logarithm of target DNA concentration and electrochemical response of the proposed electrochemical bioassay, the red curve (with AuNPs/g-C_3N_4@rGO nanocomposites) performed excellent electrochemical analytical performances than that of the blue curve (without AuNPs/g-C_3N_4@rGO nanocomposites), indicating the attributions of AuNPs/g-C_3N_4@rGO to improve the electrochemical performances of the bioassay. Additionally, the corresponding linear curve with AuNPs/g-C_3N_4@rGO nanocomposites could be described in equation I (μA) = 8.3047 + 0.3431*logc (R^2 = 0.994) with a detection limit of 8.6 aM (Mean + 3SD, Mean was the average electrochemical responses and SD was the standard deviation of blank detection, n = 3). The proposed bioassay showed favorable analytical performances for the potential application in the sensitive detection of DNA 5-methylcytosine by comparing it with some previous literatures (Table S2).

3.7. Reproducibility, stability, and specificity of the DNA biosensor

Additionally, five independent electrodes were applied to the detection of 100 pM target DNA under the same conditions to evaluate the repeatability of the proposed electrochemical bioassay. As shown in Fig. 8A, the relative standard deviation (RSD) of the repeatability evaluation was 4.54%, indicating the exceptional repeatability of the biosensor. The stability of the biosensor was evaluated by the detection of target DNA (1 nM). The electrodes were stored at 4 °C in the refrigerator and detected every week. As shown in Fig. 8B, the electrochemical response decreased gradually with store time. After 4 weeks, the biosensor was still retained around 93.7% of the original DPV response, indicating acceptable stability of the proposed bioassay. The specificity of the proposed biosensor was evaluated by using various interfering oligonucleotides, including non-complementary DNA (Mn), multi-base mismatched target DNA (Mx) and one-mismatched target DNA (M1). As shown in Fig. 8C, the target DNA (100 pM) performed a higher electrochemical response than that of the other oligonucleotides, indicating the excellent specificity of the proposed electrochemical bioassay.

Furthermore, in order to evaluate the application of the proposed electrochemical biosensor in clinical diagnosis, it was

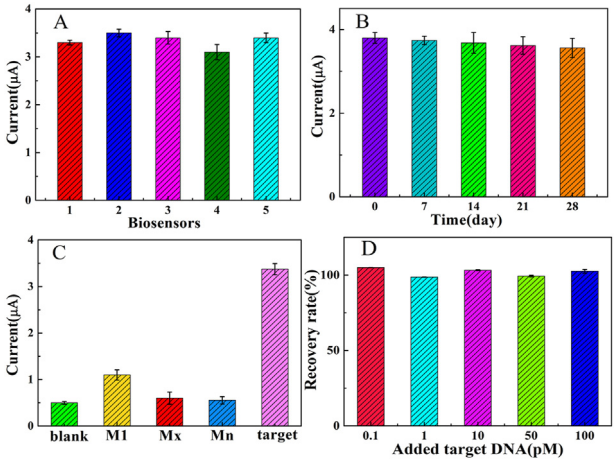

Fig. 8. (A) The reproducibility of the electrochemical biosensor; (B) the long-term storage stability of the biosensor; (C) the specificity of the platform; (D) the recovery test results of the bioassay.

employed for the detection of the DNA 5-methylcytosine in the human serum samples. Human serum samples from healthy individuals served as a complex biological system. As shown in Fig. 8D, with various concentrations of target DNA (0.1–100 pM) in the 20-fold diluted (10 mM PBS) human serum samples, the recovery rate of the added target DNA is ranged from 98.7% to 105% based on the calculation *via* proposed electrochemical bioassay, suggesting a desirable recovery performance and great promising application to clinical diagnosis.

4. Conclusion

In summary, a novel 3D matrixed DNA self-nanocatalyzer was proposed as an efficient electrochemical sensitizer for the ultrasensitive bioassay of DNA 5-methylcytosine *via* AuNPs supporting DNA self-hybridization with hemin immobilized in the G4 structure as biomimetic enzyme and MB inset in the double-stranded structure as electrochemical mediator. The proposed strategy performed a linear range from 10^{-17} M to 10^{-8} M with a detection limit of 8.6 aM. Remarkably, the successful approach of the 3D matrixed DNA self-nanocatalyzer could be easily expanded to estimate various biomarkers, including protein, DNA, phosphorylation and glycosylation, providing a promising strategy for clinical diagnosis and mechanism investigation of various diseases.

CRediT authorship contribution statement

Quanjing Zhu: Study design, Study conduct, Data analysis and

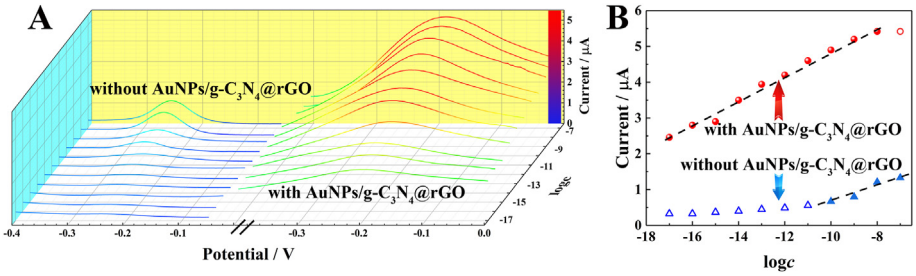

Fig. 7. (A) DPV responses of target DNA with different concentrations (10^{-17} M–10^{-7} M). (B) A linear relationship between the logarithm of DNA concentration and current signals, red curve and blue curve show the linear relationship with and without AuNPs/g-C_3N_4@rGO nanocomposites respectively. (For interpretation of the references to color in this figure legend, the reader is referred to the Web version of this article.)

interpretation. **Haoyang Yang:** Study conduct. **Jing Luo:** Study design, Study conduct. **Hui Huang:** Technical and material support. **Lichao Fang:** Data collection, Technical and material support. **Jun Deng:** Technical and material support, All authors read and approved the final version of the manuscript. **Chenghong Li:** Data collection. **Yan Li:** Study design, Data analysis and interpretation, Drafting and revising manuscript. **Tao Zeng:** Data collection, Data analysis and interpretation. **Junsong Zheng:** Study design, Drafting and revising manuscript.

Declaration of competing interest

The authors declare that they have no known competing financial interests or personal relationships that could have appeared to influence the work reported in this paper.

Acknowledgments

This work was supported by the National Natural Science Foundation of China (No. 81873982, No. 81572078and No. 81972024) and Natural Science Foundation Project of CQ CSTC (cstc2019jcyj-zdxm0037).

Appendix A. Supplementary data

Supplementary data to this article can be found online at https://doi.org/10.1016/j.aca.2020.10.064.

References

[1] G. Egger, G. Liang, A. Aparicio, P.A. Jones, Epigenetics in human disease and prospects for epigenetic therapy, Nature 429 (2004) 457–463.
[2] T.K. Kundu, M.R. Rao, CpG islands in chromatin organization and gene expression, J. Biochem. 125 (1999) 217–222.
[3] Z. Jin, Y. Liu, DNA methylation in human diseases, Genes & Diseases. 5 (2018) 1–8.
[4] D. Schubeler, Function and information content of DNA methylation, Nature 517 (2015) 321–326.
[5] R.H. Xu, W. Wei, M. Krawczyk, W. Wang, H. Luo, K. Flagg, S. Yi, W. Shi, Q. Quan, K. Li, L. Zheng, H. Zhang, B.A. Caughey, Q. Zhao, J. Hou, R. Zhang, Y. Xu, H. Cai, G. Li, R. Hou, Z. Zhong, D. Lin, X. Fu, J. Zhu, Y. Duan, M. Yu, B. Ying, W. Zhang, J. Wang, E. Zhang, C. Zhang, O. Li, R. Guo, H. Carter, J.K. Zhu, X. Hao, K. Zhang, Circulating tumour DNA methylation markers for diagnosis and prognosis of hepatocellular carcinoma, Nat. Mater. 16 (2017) 1155–1161.
[6] M.J. Ziller, K.D. Hansen, A. Meissner, M.J. Aryee, Coverage recommendations for methylation analysis by whole-genome bisulfite sequencing, Nat. Methods 12 (2015) 230–232.
[7] H.K. Hsu, Y.I. Weng, P.Y. Hsu, T.H. Huang, Y.W. Huang, Detection of DNA methylation by MeDIP and MBDCap assays: an overview of techniques, Methods Mol. Biol. 2102 (2020) 225–234.
[8] M. Labib, E.H. Sargent, S.O. Kelley, Electrochemical methods for the analysis of clinically relevant biomolecules, Chem. Rev. 116 (2016) 9001–9090.
[9] L. Krejcova, L. Richtera, D. Hynek, J. Labuda, V. Adam, Current trends in electrochemical sensing and biosensing of DNA methylation, Biosens. Bioelectron. 97 (2017) 384–399.
[10] C.M. Martinez, L.H. Alvarez, Application of redox mediators in bioelectrochemical systems, Biotechnol. Adv. 36 (2018) 1412–1423.
[11] J.L. Hammond, N. Formisano, P. Estrela, S. Carrara, J. Tkac, Electrochemical biosensors and nanobiosensors, Essays Biochem. 60 (2016) 69–80.
[12] H. Hua, Y. Liu, X. Guan, Y. Li, DNA nanosensors based on the use of single gold nanowire electrodes and Methylene Blue as an intercalator, Mikrochim. Acta 185 (2018) 152.
[13] Y. Li, H. Liu, H. Huang, J. Deng, L. Fang, J. Luo, S. Zhang, J. Huang, W. Liang, J. Zheng, A sensitive electrochemical strategy via multiple amplification reactions for the detection of E. coli O157: H7, Biosens. Bioelectron. 147 (2020) 111752.
[14] D. Zeng, H. Zhang, D. Zhu, J. Li, L. San, Z. Wang, C. Wang, Y. Wang, L. Wang, X. Zuo, X. Mi, A novel ultrasensitive electrochemical DNA sensor based on double tetrahedral nanostructures, Biosens. Bioelectron. 71 (2015) 434–438.
[15] I. Palchetti, New trends in the design of enzyme-based biosensors for medical applications, Mini Rev. Med. Chem. 16 (2016) 1125–1133.
[16] J. Yang, L. Zheng, Y. Wang, W. Li, J. Zhang, J. Gu, Y. Fu, Guanine-rich DNA-based peroxidase mimetics for colorimetric assays of alkaline phosphatase, Biosens. Bioelectron. 77 (2016) 549–556.
[17] H. Ravan, Isothermal RNA detection through the formation of DNA concatemers containing HRP-mimicking DNAzymes on the surface of gold nanoparticles, Biosens. Bioelectron. 80 (2016) 67–73.
[18] Y. Wu, L. Zou, S. Lei, Q. Yu, B. Ye, Highly sensitive electrochemical thrombin aptasensor based on peptide-enhanced electrocatalysis of hemin/G-quadruplex and nanocomposite as nanocarrier, Biosens. Bioelectron. 97 (2017) 317–324.
[19] T. Cao, F.T. Zhang, L.Y. Cai, Y.L. Zhou, N.J. Buurma, X.X. Zhang, Investigation of the interactions between methylene blue and intramolecular G-quadruplexes: an explicit distinction in electrochemical behavior, Analyst 142 (2017) 987–993.
[20] S.V. Otari, M. Kumar, M.Z. Anwar, N.D. Thorat, S.K.S. Patel, D. Lee, J.H. Lee, J. Lee, Y.C. Kang, L. Zhang, Rapid synthesis and decoration of reduced graphene oxide with gold nanoparticles by thermostable peptides for memory device and photothermal applications, Sci. Rep. 7 (2017) 10980.
[21] Q. Liu, J. Zhang, Graphene supported Co-g-C_3N_4 as a novel metal–macrocyclic electrocatalyst for the oxygen reduction reaction in fuel cells, Langmuir 29 (2013) 3821–3828.
[22] L.R. Maher, B. Wold, P.B. Dervan, Inhibition of DNA binding proteins by oligonucleotide-directed triple helix formation, Science 245 (1989) 725–730.
[23] L. Chen, X. Zeng, P. Si, Y. Chen, Y. Chi, D. Kim, G. Chen, Gold nanoparticle-graphite-like C_3N_4 nanosheet nanohybrids used for electrochemiluminescent immunosensor, Anal. Chem. 86 (2014) 4188–4195.
[24] J. Duan, S. Chen, M. Jaroniec, S.Z. Qiao, Porous C_3N_4 nanolayers@ngraphene films as catalyst electrodes for highly efficient hydrogen evolution, ACS Nano 9 (2015) 931–940.
[25] J. Liu, Y. Lu, Preparation of aptamer-linked gold nanoparticle purple aggregates for colorimetric sensing of analytes, Nat. Protoc. 1 (2006) 246–252.
[26] W. Song, H. Li, H. Liang, W. Qiang, D. Xu, Disposable electrochemical aptasensor array by using in situ DNA hybridization inducing silver nanoparticles aggregate for signal amplification, Anal. Chem. 86 (2014) 2775–2783.
[27] P. Travascio, Y. Li, D. Sen, DNA-enhanced peroxidase activity of a DNA aptamer-hemin complex, Chem. Biol. 5 (1998) 505–517.
[28] I. Lee, S. Hong, N. Lee, A. Johner, Kinetics of the triplex-duplex transition in DNA, Biophys. J. 103 (2012) 2492–2501.